

Absolute linearity measurements on a PV HgCdTe detector in the infrared

This content has been downloaded from IOPscience. Please scroll down to see the full text.

2012 Metrologia 49 S99

(<http://iopscience.iop.org/0026-1394/49/2/S99>)

View [the table of contents for this issue](#), or go to the [journal homepage](#) for more

Download details:

IP Address: 150.217.157.144

This content was downloaded on 15/05/2015 at 07:46

Please note that [terms and conditions apply](#).

Absolute linearity measurements on a PV HgCdTe detector in the infrared

Evangelos Theocharous

National Physical Laboratory (NPL), Hampton Road, Teddington, TW11 0LW, UK

E-mail: e.theo@npl.co.uk

Received 16 September 2011, in final form 9 November 2011

Published 2 March 2012

Online at stacks.iop.org/Met/49/S99

Abstract

The linearity-of-response characteristics of a photovoltaic (PV) HgCdTe detector were investigated at a number of wavelengths in the infrared, using the NPL linearity of detector response characterization facility. The measurements were performed with the test detector operating under conditions identical to those in which the detectors will be used in typical infrared radiometric applications. The deviation from linearity in the generated photocurrent was shown to be strongly dependent on the area of the detector being illuminated. Plots of the linearity factor versus generated photocurrent for different illuminated wavelengths were shown to overlap. The linearity factor was shown to be a function of the photon irradiance of the illuminating beam. This behaviour was similar to that exhibited by photoconductive (PC) HgCdTe detectors, indicating that Auger recombination was the dominant source of the deviation from linearity observed in the test detector.

(Some figures may appear in colour only in the online journal)

1. Introduction

The characterization of the linearity of response of photo-detectors is one of the most important requirements for accurate radiometry and radiation thermometry. While the linearity of response of silicon and InGaAs detectors is excellent for radiant powers of less than about 1 mW, the linearity of response of photon detectors covering longer wavelengths, such as PbS [1], PbSe [2] and photoconductive (PC) HgCdTe [3], was reported to be very poor, even for much lower incident radiant powers. The deviation from linearity of the response of these detectors was shown to be a function of irradiance rather than total radiant power incident on the active areas of these detectors. In the case of PC HgCdTe detectors, the contribution due to the thermal background radiation was shown to strongly affect the linearity characteristics of these detectors [4].

HgCdTe detectors are widely used in low-level infrared radiation measurements because they offer high D^* values in the thermal infrared region at relatively high operating temperatures. D^* or specific detectivity is a parameter which is used to quantify the ability of a detector type to measure small signals. D^* is independent of the detector active area so it provides a better parameter for comparing the performance of different detector types. D^* is equivalent to the signal to

noise ratio of a detector of unit area in a unit bandwidth when a 1 W radiant power is incident on the detector.

While the change in the output at low incident radiant power levels is expected to be proportional to the change of the incident photon flux, at higher flux levels the dependence is expected to be non-linear because the number of excess carriers is large enough to affect the total carrier density and the carrier lifetime [5]. Although the linearity characteristics of photovoltaic (PV) HgCdTe have been briefly mentioned [6], they have never been studied systematically because their active areas have been limited to diameters of 1 mm or less. However, PV HgCdTe detectors with 2 mm diameter active areas are now being fabricated, albeit with very low shunt resistance values. The indications are that the linearity-of-response characteristics of PV HgCdTe detectors are superior to those of PC HgCdTe detectors, hence their widespread use in Fourier transform (FT) spectrometry to cover the 5 μm to 12 μm wavelength range.

The purpose of this paper is to report the results of an investigation carried out at NPL into the absolute linearity of response characterization of a PV HgCdTe detector with a 2 mm diameter active area. To the best of our knowledge, this is the first reported study of the absolute linearity characteristics of a PV HgCdTe detector.

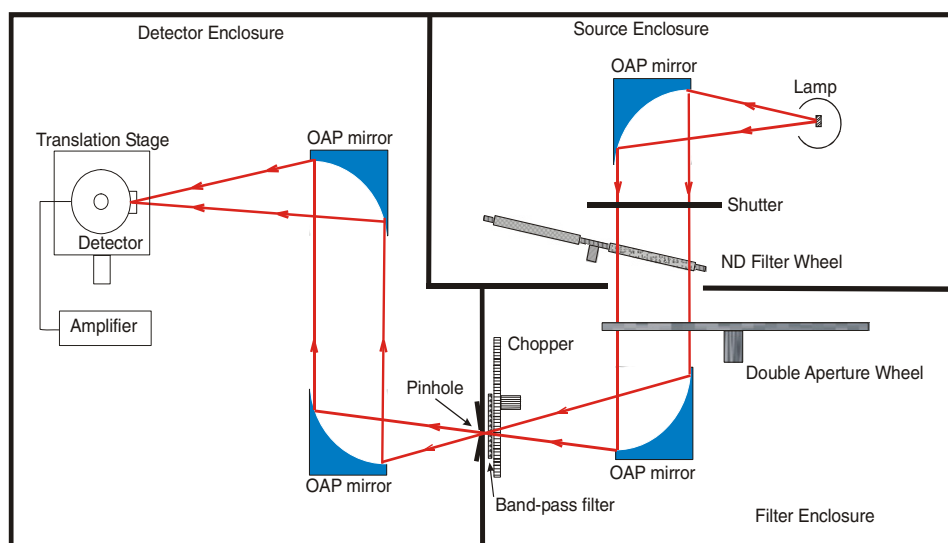


Figure 1. Schematic diagram of the layout of the NPL linearity measurement facility.

2. Apparatus and method

The NPL linearity-of-response measurement facility was used to characterize the linearity of response of the test detector at three different wavelengths, 10.3 μm , 4.7 μm and 2.2 μm . A schematic diagram of the facility is shown in figure 1. Two radiation sources were used: a tungsten strip lamp with a sapphire window was used for wavelengths up to 5 μm while a Nernst glower source was used for longer wavelengths. A fraction of the radiation emitted by the source is collimated by an off-axis parabolic (OAP) mirror. The collimated radiation passed through two rotational discs and was imaged onto a pinhole/field stop by the second identical OAP mirror. The first disc was a filter wheel containing ten reflective neutral density filters deposited on ZnSe substrates. The neutral density filters attenuated the beam in optical density steps of approximately 0.3. The filter wheel was positioned at an angle to the collimated beam to avoid inter-reflections between optical components. The second disc was the double-aperture wheel [7] which included the apertures A, B and A+B. The surface of this disc was blackened with a paint which had low reflectance in the infrared. Both rotational discs were driven by PC-controlled stepper motors. The radiant flux incident on the detector was varied by introducing neutral density filters of different transmission because this method was considered superior to changing the sizes (diameters) of apertures A and B, since the latter approach also changed the effective F/number of the beam incident on the detector being tested.

The radiant power was modulated by a two-slot mechanical chopper located in front of the pinhole. Narrow band-pass filters were installed just before the pinhole in order to select quasi-monochromatic radiation of the appropriate wavelength. The test detector was mounted on a three-axes translation stage. This allowed the real image of the pinhole to be focused on the active surface of the test detector using a pair of identical, optically polished OAP mirrors (F/3.5, 50 mm diameter aperture). The photocurrent generated by

the PV HgCdTe detector was amplified by a dedicated trans-impedance amplifier and gains of 10^4 and 10^5 V A^{-1} were used during this evaluation. The amplified output was fed into a digital lock-in amplifier for rectification. The operation of the facility and data gathering were fully automated.

The linearity factor $L(V_{A+B})$ represents a measure of the linearity of response of a photodetection system for an output of $(V_A + V_B)/2$ and its value is given by

$$L(V_{A+B}) = \frac{V_{A+B}}{V_A + V_B} \quad (1)$$

where V_A , V_B and V_{A+B} represent the zero-corrected output signals when apertures A, B and A+B were open, respectively, with V_A set to be approximately equal to V_B . A detection system is said to have a linear response when the value of $L(V_{A+B})$ is equal to unity. Where $L(V_{A+B})$ deviates from unity, it can be used to estimate correction factors to apply for different detector output signals to transfer the absolute responsivity calibration from one detector output signal level to another [8].

The test detector had a 2 mm diameter active area and was mounted inside a side-looking liquid nitrogen-cooled cryogenic Dewar for operation at 77 K. The Dewar was fitted with an anti-reflection (AR) coated ZnSe window. The Dewar incorporated a cold field-stop which restricted the detector field of view (FOV) to approximately 60° (full angle) to limit the noise contribution due to the thermal background radiation [9]. Using the NPL infrared spectral responsivity measurement facility [10], the absolute spectral responsivity of the PV HgCdTe detector/transimpedance amplifier combination was measured at the wavelengths at which linearity measurements were performed. This allowed the output voltage signals to be converted to incident absolute radiant power or irradiance values. The spatial uniformity of response of the same detector was also measured on the NPL spatial uniformity-of-response measurement facility [10] in order to identify any correlation between detector linearity-of-response and

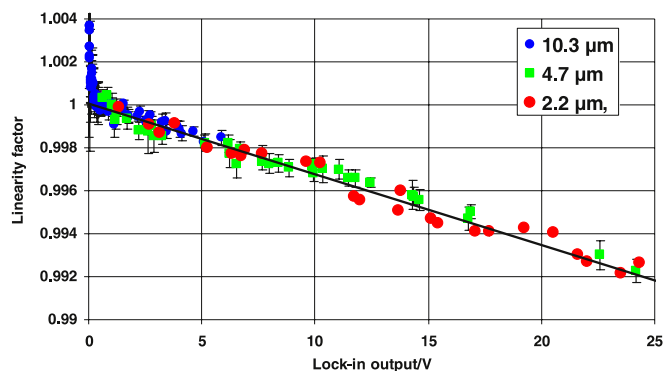


Figure 2. Linearity factor of the PV HgCdTe detector versus lock-in output, measured at 10.3 μm , 4.7 μm and 2.2 μm . Error bars shown in this and subsequent figures represent the standard deviation of at least eight repeated measurements.

the spatial uniformity-of-response characteristics of the test detector. A 70 Hz modulation frequency was used for all measurements described in this document.

The position of the probe spot on the active area of the test detector was set by viewing the illuminated area with a low power microscope (with the infrared band-pass filter removed so the unfiltered output of the tungsten filament source was transmitted). An automated procedure was then used which scanned the detector in a vertical and horizontal direction to identify its edges and therefore place the image of the pinhole at the geometric centre of the active area of the test detector.

3. Results

Figure 2 shows the plot of the linearity factor (as defined by equation (1)) of the PV HgCdTe detector measured with the active area of the test detector overfilled, at three different wavelengths, 10.3 μm , 4.7 μm and 2.2 μm . Also shown in figure 2 is the best straight line fit to the measurements taken at 2.2 μm . All data were normalized to a 10^5 V A^{-1} trans-impedance amplifier gain and 1 V lock-in amplifier sensitivity setting. The good overlap of the three plots shown in figure 2 corresponding to the three different wavelengths indicates that the wavelength of the incident radiation is not a factor when the data are plotted as a function of the lock-in output. Since the generated photocurrent is directly proportional to the lock-in amplifier output, plots of the linearity factor as a function of generated photocurrent at different wavelengths are also expected to overlap. This behaviour is similar to that observed in PC HgCdTe detectors [3].

Figure 3 shows the data shown in figure 2 but plotted as a function of dc equivalent [11] radiant power incident on the detector. Also shown in figure 3 are the corresponding best straight line fits to the data acquired at 4.7 μm and 2.2 μm . Figure 3 shows that the three plots corresponding to the three different wavelengths do not overlap. This behaviour indicates that the non-linearity arises after the photons have been converted to photoelectrons and provides evidence that the non-linearity is due to Auger recombination of the photo-generated charges [3].

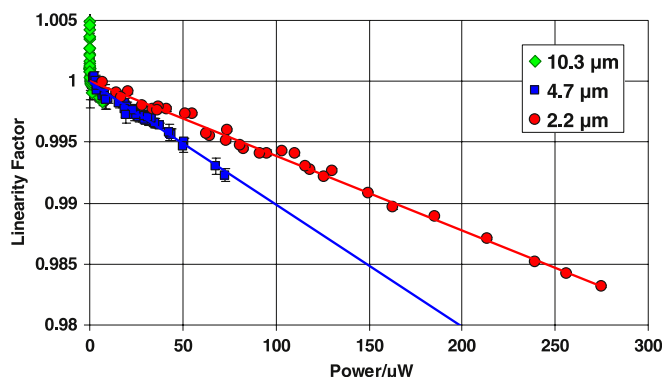


Figure 3. Plots of the linearity data as a function of total radiant power incident on the test detector. The plots corresponding to different wavelengths no longer overlap.

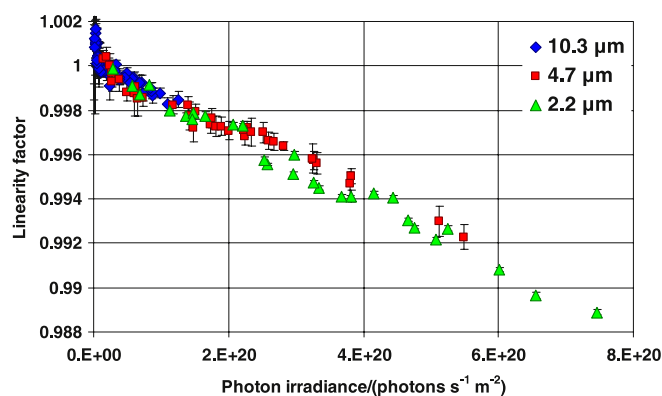


Figure 4. Plots of the linearity factor as a function of photon irradiance incident on the test detector.

Photon irradiance, E_p , is related to irradiance (radiant areance), E_e , by the equation

$$E_p = \frac{\lambda E_e}{hc} \quad (2)$$

where λ is the wavelength of the radiation, h is the Planck constant and c is the speed of light. Figure 4 shows the same data plotted as a function of photon irradiance incident on the detector where the three plots corresponding to the three different wavelengths overlap. This observation should not be surprising because the density of charged carriers produced is directly proportional to the incident photon irradiance. This behaviour is identical to that observed in PC HgCdTe detectors [3] and provides further evidence that the observed non-linearity is due to Auger recombination of the photo-generated charges [5].

Figure 5 shows the data shown in figure 2 plotted on a logarithmic abscissa. Also shown in figure 5 is the best straight line fit to the measurements taken at 2.2 μm . Figure 5 shows that for small lock-in amplifier outputs (output less than 0.1 V) the test detector exhibits a super-linear response. The origin of this super-linear response is currently unknown. This, in combination with the deviation from linearity observed for high lock-in amplifier outputs (output higher than about 10 V), shows that the dynamic range of the test detector is very low (less than 100).

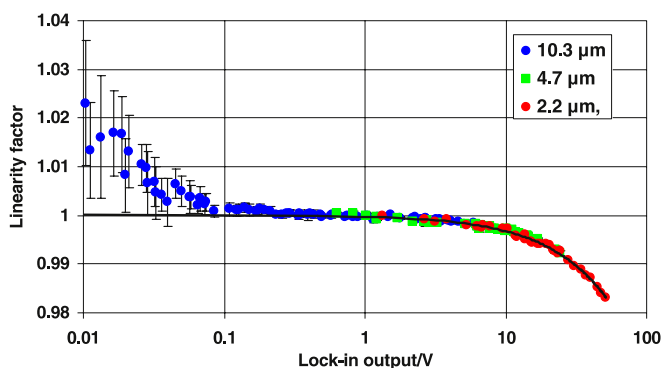


Figure 5. Linearity factor of the PV HgCdTe detector versus lock-in output, measured at 10.3 μm , 4.7 μm and 2.2 μm plotted with a logarithmic abscissa.

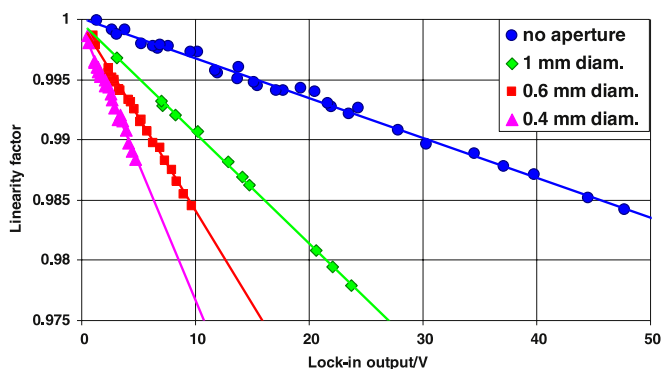


Figure 6. The linearity factor of the PV HgCdTe detector measured at 2.2 μm as a function of lock-in amplifier output, measured with 0.4 mm, 0.6 mm and 1.0 mm diameter spots, as well as with the active area of the test detector overfilled.

In previous studies, the low spectral radiance available from thermal sources around 10 μm prevented a full evaluation of the linearity-of-response characteristics of detectors responding to these long wavelengths. The realization that the linearity characteristics of the PV HgCdTe detector are independent of wavelength allows the measurements to be repeated at shorter wavelengths where the spectral radiance available from thermal sources is much higher. The linearity factor of the PV HgCdTe detector was measured at 2.2 μm with different areas of the test detector being illuminated. Measurements of the linearity factor were completed with 0.4 mm, 0.6 mm and 1.0 mm diameter spots as well as with the active area of the test detector overfilled and the results are plotted in figure 6. Also shown in figure 6 are the best straight line fits to the measurements corresponding to each illumination condition. Figure 6 shows that the plots of the linearity factor versus lock-in amplifier output, completed with different areas being illuminated, have very different slopes. This confirms that the area of the test detector being illuminated plays an important role in the magnitude of the non-linearity observed.

The data shown in figure 6 were re-plotted so that the linearity factor is plotted as a function of the incident spectral irradiance (microwatt per unit area) illuminating the test detector and the results are shown in figure 7. Also shown in figure 7 are the best straight line fits to the measurements

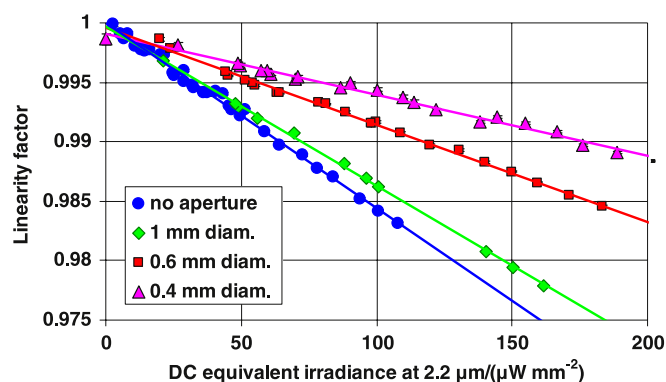


Figure 7. The linearity factor of the test detector measured at 2.2 μm as a function of the dc equivalent irradiance. Measurements were carried out with 0.4 mm, 0.6 mm and 1.0 mm diameter spots, as well as with the active area of the test detector overfilled.

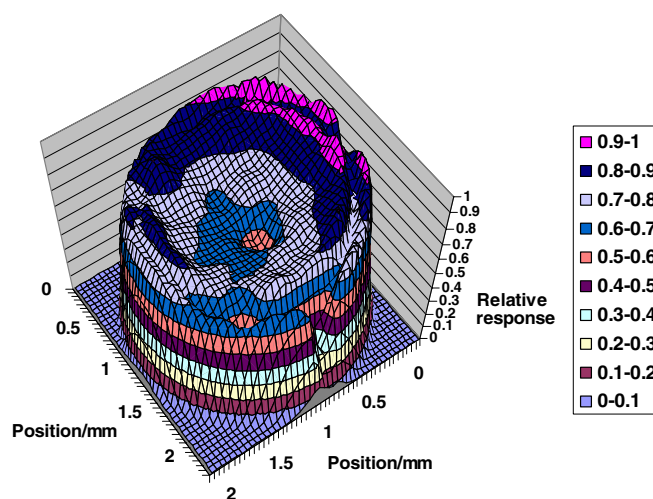


Figure 8. Spatial uniformity of response of the PV HgCdTe detector at 2.2 μm , measured using a 100 μm diameter probe spot.

corresponding to each illumination condition. Although the overlap of the four plots shown in figure 7 is better than the overlap of the plots shown in figure 6, it is still poor. When the corresponding graphs were plotted for other detectors (PbS, PbSe, PC HgCdTe and pyroelectric detectors), the overlap of the plots corresponding to different illuminated areas was far superior.

When plots similar to those in figure 7 were plotted for DLATGS pyroelectric detectors [12], the same behaviour was observed, i.e. plots of the linearity factor versus irradiance, corresponding to different active areas being illuminated, did not overlap. The reason for the different slopes in the case of the DLATGS detectors was identified as the spatial non-uniformity-of-response over the active area of the DLATGS detector [12]. The spatial uniformity-of-response of the PV HgCdTe detector was measured in order to confirm the origin of the non-overlapping plots in figure 7. Figure 8 shows the spatial uniformity of response of the PV HgCdTe detector, generated at 2.2 μm by scanning a 100 μm diameter probe spot over the active area of the test detector. Figure 8 shows that the responsivity of the test detector at the centre is almost 50% of the response near the edge of the test detector. Similar spatial

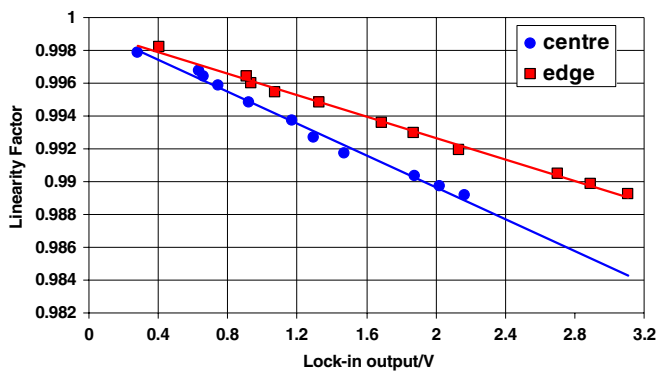


Figure 9. Plots of the linearity factor as a function of lock-in output at $2.2\ \mu\text{m}$ with a spot diameter of $0.4\ \text{mm}$, measured at the centre and near the edge of the active area of the test detector.

uniformity-of-response profiles were also measured at $10.3\ \mu\text{m}$ and $4.7\ \mu\text{m}$. The spatial uniformity-of-response profile of this detector is typical of large active area PV infrared detectors. As the shunt resistance of these detectors is reduced, it becomes comparable to the series resistance. This means that the photo-generated charges can be lost before they can be collected by the ring electrode around the circumference of the detector. Charges generated at the centre have farthest to travel and are more likely to be lost before they are collected, hence the minimum measured response at the centre of the detector active area. The presence of such large variations in the responsivity of the test detector across its active area means that as the diameter of the spot increases, it illuminates regions of the active area of the detector of higher responsivity, giving rise to higher lock-in amplifier outputs for the same level of incident irradiance. The large variations in the responsivity across the active area of the test detector can account for the difference in the slopes of the plots of the linearity factor versus irradiance seen in figure 7.

In order to provide further confirmation of the importance of spatial uniformity of response to the linearity characteristics of the test detector, the linearity factor of the PV HgCdTe detector was measured at $2.2\ \mu\text{m}$ using a $0.4\ \text{mm}$ diameter spot illuminating the geometric centre of the active area of the detector. Without altering the spectral irradiance within the spot (i.e. same lamp current), measurements were repeated when the same $0.4\ \text{mm}$ diameter spot was illuminating a position near the edge of the active area of the test detector. Figure 9 shows the plots of the linearity factor as a function of lock-in amplifier output measured at the centre and near the edge of the active area of the test detector, along with the best straight lines fits to the two sets of data. The slopes of the two plots are different. The difference in the slopes confirms the importance of the spatial non-uniformity of response in the characterization of the linearity of response of photodetectors. This effect can give rise to the non-overlapping plots shown in figure 7.

4. Discussion

When a beam of optical radiation of uniform spectral irradiance illuminates a well-defined area on the PV HgCdTe detector,

photocharges are generated which are normally collected and represent the generated photocurrent. The magnitude of the photo-generated current at any given wavelength should be proportional to the irradiance of the beam illuminating the photodetector. However, unless the photo-generated charge carriers are removed, there is a likelihood they can destroy each other by Auger recombination. Auger recombination, therefore, results in the destruction of some of these photo-generated charges. The number of photo-generated charges which are lost due to Auger recombination depends on the density of the photo-generated charges [13]. For this reason, when an incident beam of cross sectional area A and radiant power P is focused tighter so the area illuminated on the detector is halved, the density of the photo-generated charges doubles, which increases the probability of Auger recombination and thus increases the non-linearity observed. It is clear that the deviation from linearity (and hence the linearity factor) is governed by the photon irradiance incident on the detector and, indeed, this is confirmed by the overlap of the plots shown in figure 4. This behaviour is identical to that observed in PC HgCdTe detectors [3].

However, the plots of the linearity factor versus photon irradiance (shown in figure 7) corresponding to different illuminated areas do not overlap. The reason for the non-overlap is the very large variation in the responsivity of the test detector across its active area (spatial uniformity of response). In the case of the PV HgCdTe detector, the response at its geometric centre is only half of the response near the edge of the active area of the test detector (see figure 8). As the diameter of the illuminating spot increases, regions of the active area of higher responsivity are illuminated, so the effective responsivity of the test detector depends on the diameter of the illuminating spot. This gives rise to the non-overlapping plots shown in figure 7.

For the measurement of the linearity of response, as well as for other radiometric measurements using the PV HgCdTe detector, a transimpedance amplifier and a lock-in amplifier are required to amplify and rectify the detector output. The observed non-linearity could therefore arise from one or more of the test detector, the transimpedance amplifier or the lock-in amplifier. It is often difficult to separate the non-linearity contributions due to the detector and the two amplifiers. The linearity of the transimpedance amplifier was checked by feeding electric currents of known value and measuring the amplifier output. The non-linearity of the trans-amplifier was insignificant at the gain settings and outputs that were used in the PV HgCdTe linearity evaluation. This transimpedance amplifier has been selected to match the characteristics of the test detector and has been assigned to the PV HgCdTe detector under test and the two will be used in the future as a unit. The linearity factor of the lock-in amplifier was measured using the 'subtraction method' [14] which showed that the linearity factor of the lock-in amplifier never deviated from unity by more than 0.1% . This confirms that the observed non-linearity is due to the PV HgCdTe detector.

The linearity characteristics of the PV HgCdTe detector were measured with the test detector operating in a configuration identical to the one in which the detector will

be used in a typical infrared radiometric application, i.e. with the radiation incident on the detector modulated by a modulator such as a mechanical chopper, the detector output amplified by its own dedicated amplifier and rectified by a digital lock-in amplifier. Furthermore, the 'radiometric zero' was defined by blocking the infrared source output by a shutter maintained at ambient temperature and coated with a paint which had low reflectance in the infrared (total hemispherical reflectance approximately 5% at 10.3 μm). This is identical to the way the radiometric zero would be defined in a typical infrared radiometric measurement [11]. It should be pointed out that this method of defining radiometric zero will not be acceptable in infrared spectro-radiometric measurements because, with the shutter closed, there is still a significant amount of radiant power generated by the shutter which reaches the detector [15]. Finally, the linearity characterization was completed with everything in the FOV of the test detector set at ambient temperature. Theocharous and Theocharous [4] showed that the density of the photo-generated charges produced by the thermal background is over an order of magnitude higher than that generated by the incident (modulated) radiant signal. Since Auger recombination cannot discriminate between photo-generated charges produced by the thermal background and those produced by the modulated signal, we find that the thermal background can be the dominant factor in the determination of the linearity factor of the test detector. It is therefore important to stress that the non-linearity characteristics of the test detector reported in this document are only valid when objects in its FOV are maintained at 20 °C. This is the measurement condition under which PV HgCdTe detectors normally operate. In a separate experiment we have also shown that the introduction of cold band-pass filters [15] or the reduction of the FOV of the test detector resulted in a reduction of the thermal background radiation reaching the test detector which, in turn, increased the range of incident photon irradiance values over which the response of the PV HgCdTe detector remained linear.

5. Conclusions

The linearity characteristics of a PV HgCdTe detector were experimentally investigated in the infrared wavelength region using the NPL linearity-of-response characterization facility. The measurements were performed with the test detector operating under conditions identical to those in which the detectors will be used in typical infrared radiometric applications. The NPL linearity-of-response characterization facility is based on the double-aperture method and provided absolute linearity measurements for these detection systems. The non-linearity of the PV HgCdTe detectors was shown to be a function of photon irradiance rather than the total radiant power incident on the test detector. This implies that by operating these detectors with their active areas overfilled, their linear range of operation in terms of incident radiant

power increases. NPL operates PV and PC HgCdTe detectors in association with integrating spheres, which results in the elimination of the effects arising from their spatial non-uniform response as well as the extension of their linear range of operation [11].

Acknowledgments

© Crown copyright 2011. Reproduced by permission of the Controller of HMSO and the Queen's printer for Scotland. This work was funded by the National Measurement Office of the United Kingdom Department for Business, Innovation and Skills.

References

- [1] Theocharous E 2006 Absolute linearity measurements on PbS detectors in the infrared *Appl. Opt.* **45** 2381–6
- [2] Theocharous E 2007 Absolute linearity measurements on a PbSe detector in the infrared *Infrared Phys. Technol.* **50** 63–9
- [3] Theocharous E, Ishii J and Fox N P 2004 Absolute linearity measurements on HgCdTe detectors in the infrared *Appl. Opt.* **43** 4182–8
- [4] Theocharous E and Theocharous O J 2006 Practical limit of the accuracy of radiometric measurements using HgCdTe detectors *Appl. Opt.* **45** 7753–9
- [5] Bartoli J, Allen R, Esterowitz L and Kruer M 1974 Angular-limited carrier lifetimes in HgCdTe at high excess carrier concentrations *Appl. Phys.* **45** 2150–4
- [6] Theocharous E, Ishii J and Fox N P 2005 A comparison of the performance of a photovoltaic HgCdTe detector with that of a large area single pixel QWIP for infrared radiometric applications *Infrared Phys. Technol.* **46** 309–22
- [7] Mielenz K D and Eckerle K L 1972 Spectrophotometer linearity testing using the double aperture method *Appl. Opt.* **11** 2294–303
- [8] Sanders C L 1972 Accurate measurements of and corrections for nonlinearities in radiometers *J. Res. Natl Bur. Stand. A* **76** 437–53
- [9] Theocharous E and Birch J R 2002 Detectors for mid- and far-infrared spectrometry: selection and use *Handbook of Vibrational Spectroscopy* ed J M Chalmers and P R Griffiths (Chichester: Wiley) pp 349–67
- [10] Theocharous E, Clarke F J J, Rogers L J and Fox N P 2003 Latest measurement techniques at NPL for the characterization of infrared detectors and materials *Proc. SPIE* **5209** 228–39
- [11] Theocharous E, Prior T R, Haycocks P R and Fox N P 1998 High accuracy, infrared spectral responsivity scale *Metrologia* **35** 543–8
- [12] Theocharous E 2008 Absolute linearity measurements on a gold-black-coated deuterated L-alanine-doped triglycine sulphate pyroelectric detector *Appl. Opt.* **47** 3731–6
- [13] Lundstrom M 2000 *Fundamentals of Carrier Transport* 2nd edn (Cambridge: Cambridge University Press)
- [14] Theocharous E 2008 Absolute linearity calibration of lock-in amplifiers *Appl. Opt.* **47** 1090–6
- [15] Theocharous E, Fox N P, Sapritsky V I, Mekhontsev S N and Morozova S P 1998 Absolute measurements of blackbody emitted radiance *Metrologia* **35** 549–54